Supplementary Information (SI) for RSC Advances.
This journal is © The Royal Society of Chemistry 2025

Supplementary Data

Ultra-Sensitive Low-Frequency Dual-Mode Humidity Sensor Using a Methyl Red–PVA–Graphene Oxide Composite

Mushahid Hussain [a,b,1,*], Nadir Ali Khan [a], Wei-Chun Lin [b], Muhammad Yaseen [c], Fakhra Aziz [a], Muhammad Ali [d], Naseem Abbas [e,1]

[a] *Department of Electronics, University of Peshawar, Peshawar, 25120, Pakistan*

[b] *Department of Photonics, National Sun Yat-sen University, No. 70, Lianhai Rd., Gushan Dist., Kaohsiung, Taiwan, ROC*

[c] *Department of Chemistry, Division of Science & Technology, University of Education, Lahore, Pakistan*

[d] *Department of Physics, University of Peshawar, Peshawar, 25120, Pakistan*

[e] *Department of Mechanical Engineering, Sejong University, Seoul, 05006, Republic of Korea*

[1] *Authors are equally contributed to this work.*

***Corresponding:** mushahidhussain708@gmail.com (M.H)

Table of Contents

Pristine PVA Figure S1(a-b) display a semicrystalline polymeric texture with smooth morphology. The Figure S1 (c-d) exhibits irregular granular surface morphology with randomly distributed micro-aggregates. The graphene oxide (GO) sheet structure showing oxygen-containing functional groups (hydroxyl, epoxy, and carboxyl) on the basal plane and edges with highly porous structure in Figure S1 (e-f). These functional groups enhance water molecule adsorption, enabling high sensitivity in humidity sensing applications.

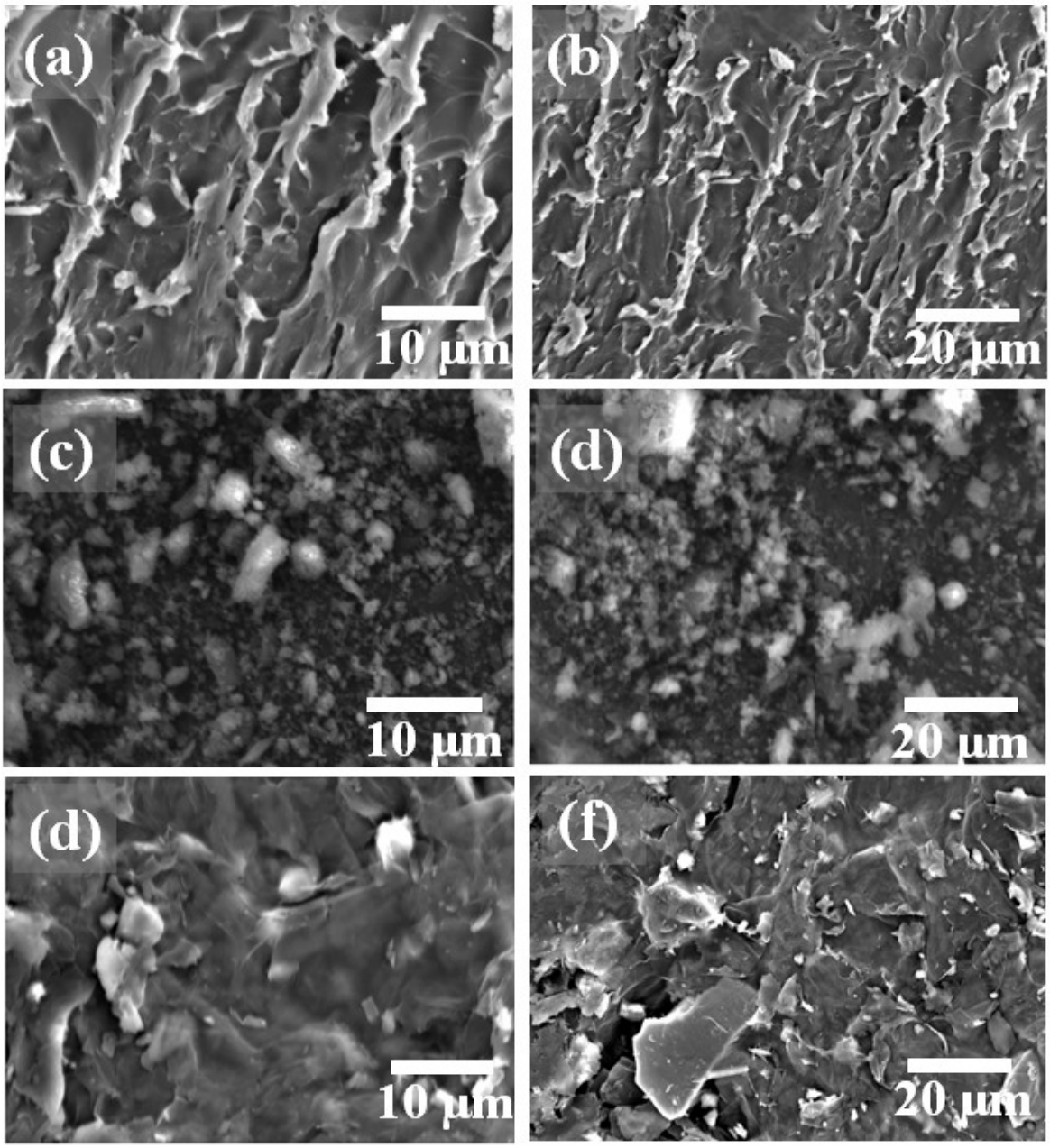

Figure S1: SEM micrographs of **(a)** pristine PVA at 10 µm **(b)** at 20 µm, (c) pristine MR at 10 µm (d) at 20 µm, and (e) pristine GO at 10 µm (f) 20 µm

Stability performance of the MPG composite humidity sensor over five consecutive days at different relative humidity (RH) levels measured at 100 Hz. Figure S2 capacitance and resistance responses remain stable with minimal fluctuations across all tested RH conditions, indicating excellent repeatability and short-term operational reliability of the sensor.

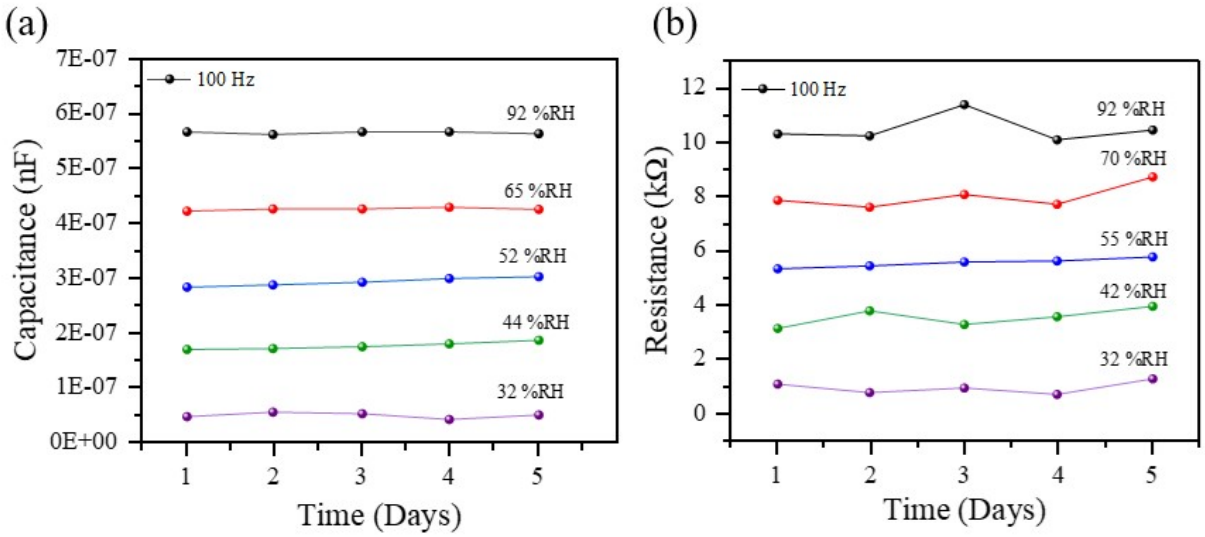

Figure S2: Stability of MPG humidity sensor over time (a) Capacitive-type humidity sensor (b) Resistive-type humidity sensor

Real-time monitoring of human respiration using the MPG composite humidity sensor. The sensor clearly distinguishes between normal breathing (0–200 s) and fast breathing (200–400 s) through periodic response oscillations corresponding to inhalation (lower response) and exhalation (higher response). The distinct frequency shift between the two breathing modes demonstrates the sensor's high sensitivity, fast response, and potential application in wearable healthcare devices for respiratory monitoring.

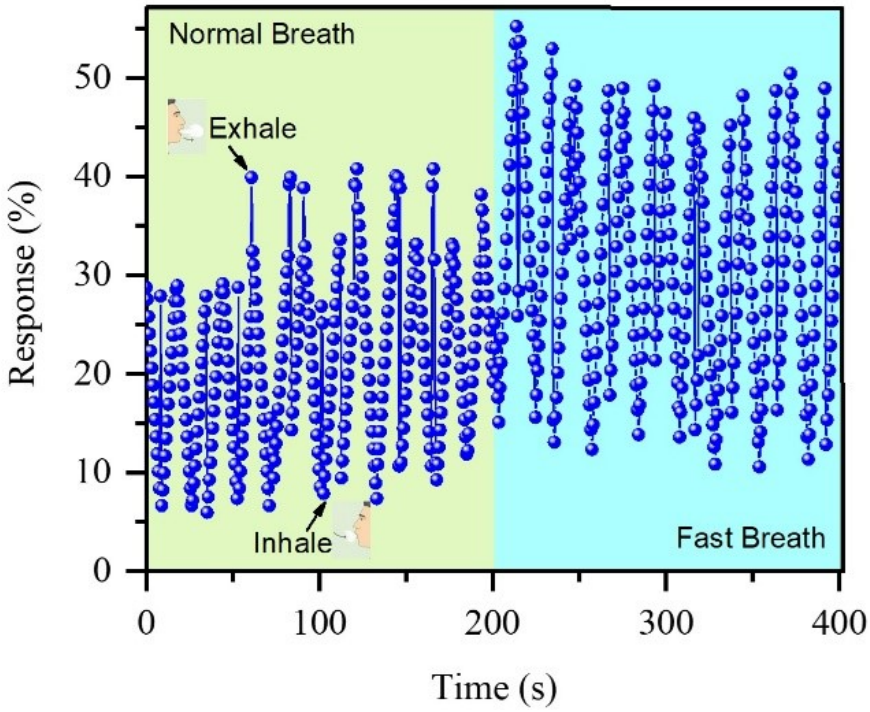

Figure S3: Real-time humidity response of the MPG sensor under human breathing. Peaks indicate exhalation (humid air), valleys indicate inhalation (dry air)

Schematic diagram of the interdigitated electrode (IDE) structure used for the MPG composite humidity sensor. The IDE consists of silver electrodes deposited on an alumina substrate with finger width and spacing of 0.21 mm, an active electrode length of 4 mm, and total device dimensions of 14 mm × 7 mm. This design provides a large effective sensing area, enabling efficient interaction between the sensing film and ambient humidity.

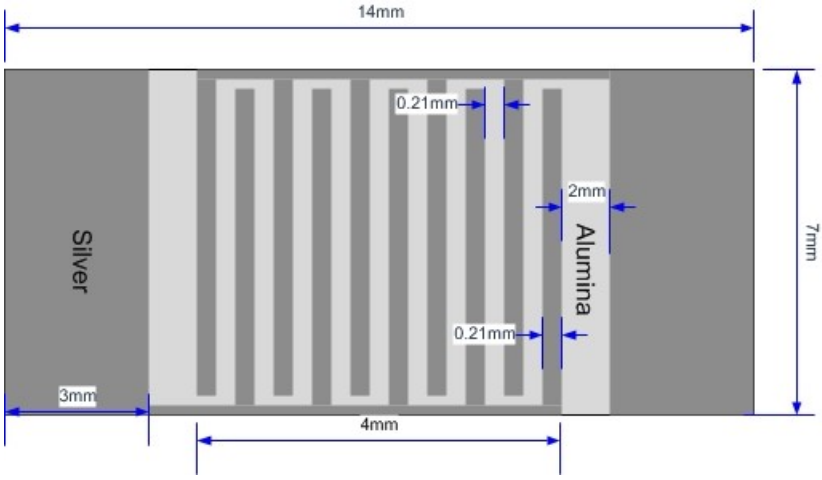

Figure S4: Schematic view of an interdigitated alumina electrode (IDE) for a humidity sensor

The FTIR spectra of the individual components—methyl red (MR), polyvinyl alcohol (PVA), and graphene oxide (GO) reveal their characteristic functional groups. MR exhibited a broad O–H stretching band at 3447.6 cm^{-1}, alongside distinct C=O stretching at 1728.1 cm^{-1}, aromatic C=C stretching near 1604.9 cm^{-1} and 1491.3 cm^{-1}, and the N=N azo stretching around 1373.2 cm^{-1}. GO, in turn, shows strong O–H vibrations at 3337.9 cm^{-1}, C=O stretching at 1733 cm^{-1}, and C–O stretching around 1049 cm^{-1}, all indicative of its oxidized and functionalized graphene backbone. PVA is marked by a pronounced O–H stretch at 3358 cm^{-1} and C–H stretching near 2974.4 cm^{-1}, consistent with its polymeric alcohol nature (Figure S5).

Upon forming the MPG composite, significant shifts and slight intensity variations are observed in these bands, suggesting extensive intermolecular interactions. The broad O–H stretching band moved to a lower wavenumber (3304.1 cm^{-1}) compared to both PVA and GO, reflecting the establishment of hydrogen bonding networks among the –OH groups of PVA, residual hydroxyls of GO, and possibly the carboxyl functionalities. The C=O stretching vibration shifted from 1733 cm^{-1} in GO and 1728.1 cm^{-1} in MR to 1708.5 cm^{-1} in the composite MPG, indicating that carbonyl

groups are engaged in hydrogen bonding or dipole–dipole interactions, which weakens the C=O bond and lowers its stretching frequency (Figure S5).

The C–N and N=N peaks of MR (originally at 1277 cm^{-1} and 1373.2 cm^{-1}) also shifted slightly downwards in the composite (1270.4 cm^{-1} and 1360.7 cm^{-1}), suggesting that electrostatic or donor–acceptor interactions occurred between the electron-rich azo nitrogen and oxygen-containing groups on GO or the hydroxyls in PVA. Additionally, the aromatic C–H out-of-plane deformation peak shifts from 816.5 cm^{-1} in MR and 873 cm^{-1} in GO to 809 cm^{-1} in the composite, consistent with subtle changes in the conjugated aromatic environment and possible π–π stacking between MR and GO sheets (Figure S5).

Collectively, these observations provided strong evidence that the MPG composite is stabilized through a combination of hydrogen bonding, π–π stacking, and donor–acceptor interactions. Hydrogen bonds mainly arise among the hydroxyl groups of PVA and GO, as well as between C=O and O–H groups, while π–π interactions are likely established between the aromatic rings of methyl red and the sp^2 domains of graphene oxide. Such synergistic interactions not only contribute to structural integrity but can also modulate the composite's electronic and sensing properties.

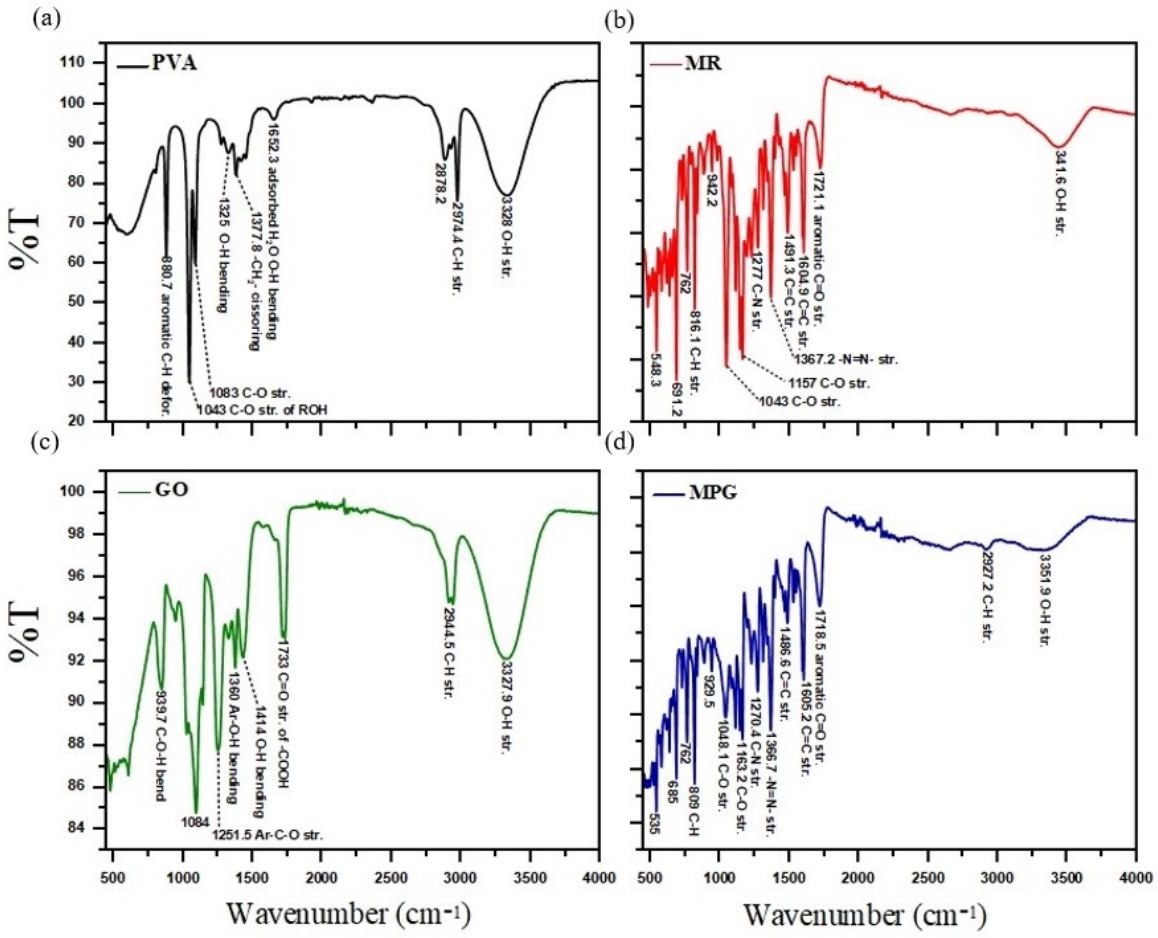

Figure S5: FTIR analyses of MR, PVA, GO stand-alone, MPG composite

Table S1: FTIR of MR, PVA, GO and MPG composite

MR (cm^{-1})	PVA (cm^{-1})	GO (cm^{-1})	MPG (cm^{-1})	Functional
3447.6	3358	3337.9	3304.1	-OH
-	2974.4	2944.5	2927.2	-CH
1728.1	-	1733	1728.5	-C=O
1604.9	-	-	1605.2	C=C
1491.3	-	1461	1480.6	C=C
1373.2	-	-	1360.7	-N=N-

1277	-	-	1270.4	C-N
1157	-	-	1163.2	C-O
1049	1040	-	1048.1	C-O
816.5	880.7	873	809	Ar.-H

The crystalline structures of MR, PVA, GO stand-alone, and MPG composite were investigated using an X-ray diffractometer as presented in Figure S6(a). The characteristic peaks of the MPG at 13.7°, 16.9°, 24.9°, and 31.6° are due to the structure of the MR moiety. The peak at 26.3° in the GO pattern advocates the presence of carbon-based elemental composition and internal carbon atoms. The weak peak at 24.6° in the XRD pattern of MPG, as shown in the figure, indicates that GO is well-dispersed within the PVA matrix. It further implies that PVA is intercalated into the inter-layers of the GO, suggesting profound dissemination of GO into the PVA matrix on a molecular level. Our results corroborate with the previously published reports[8]. It can be observed from the figure that MR remains dominant in the MPG composite. Scherrer's equation was employed to find the crystallite size.

The electronic absorption spectra of PVA, GO, MR, and their composite (MPG) were recorded to investigate the changes in electronic transitions upon composite formation. The spectral features of each individual component were altered significantly in the composite spectrum, indicating successful integration and strong electronic coupling among the constituents Figure S6(b). Methyl red exhibited its primary absorption band at wavelengths around 200 nm, beyond which the intensity declined rapidly. This high-energy absorption, though not fully resolved due to instrumental cut-off, could be attributed to $\pi \rightarrow \pi^*$ transitions originating from the conjugated aromatic system of MR. A broad, weak absorption feature extending from ~350 to ~550 nm was also observed, which was assigned to $n \rightarrow \pi^*$ transitions involving nonbonding electrons on heteroatoms, such as nitrogen in the azo linkage (–N=N–) and oxygen in carboxylic groups. The absence of any distinct peak in the 250–260 nm range indicated that the $\pi \rightarrow \pi^*$ transitions in MR occurred at higher energy levels. Polyvinyl alcohol displayed a sharp absorption peak around 270

nm, corresponding to $n \rightarrow \pi^*$ transitions associated with hydroxyl groups. As expected for a non-conjugated polymer, no significant absorption was observed in the visible region. While PVA itself is optically inactive in the longer wavelength range, its hydroxyl groups may have facilitated hydrogen bonding with MR and GO in the composite, contributing to structural stabilization and modulating electronic interactions. Graphene oxide exhibited two primary features: a strong absorption band at ~230 nm, attributed to $\pi \rightarrow \pi^*$ transitions of C=C bonds in the aromatic sp^2 domains, and a shoulder near 290 nm corresponding to $n \rightarrow \pi^*$ transitions of C=O or C–OH groups. These transitions reflected the partially conjugated and oxidized nature of GO, and its ability to engage in donor–acceptor interactions with other molecular systems. In the composite (MPG) spectrum, a substantial reorganization of absorption features was observed. A broad and intense absorption band appeared in the visible region, centered around 497 nm, which was absent in the spectra of the individual components. This new band likely arose from strong electronic interactions—specifically, charge-transfer transitions—between methyl red and graphene oxide. The π-electron-rich MR may have interacted with the π-deficient GO domains through π–π stacking or electron donor–acceptor interactions, forming a new electronic state that allowed for lower-energy transitions. Additionally, PVA may have supported this interaction through hydrogen bonding, improving the dispersion and proximity of the molecular species. The emergence of this red-shifted, high-intensity band suggested the formation of a new ground-to-excited state transition in the composite system, characterized by enhanced electron delocalization and a narrowed energy gap. These changes confirmed that the optical properties of the composite were not merely a sum of its components, but rather a result of synergistic interactions at the molecular level. In conclusion, the UV–Visible spectral analysis confirmed that the formation of the MPG composite resulted in a significant modification of electronic transitions, particularly through charge-transfer and π–π interactions. These spectral changes supported the successful fabrication of a new hybrid material with potential application in optical, sensing, or photonic technologies.

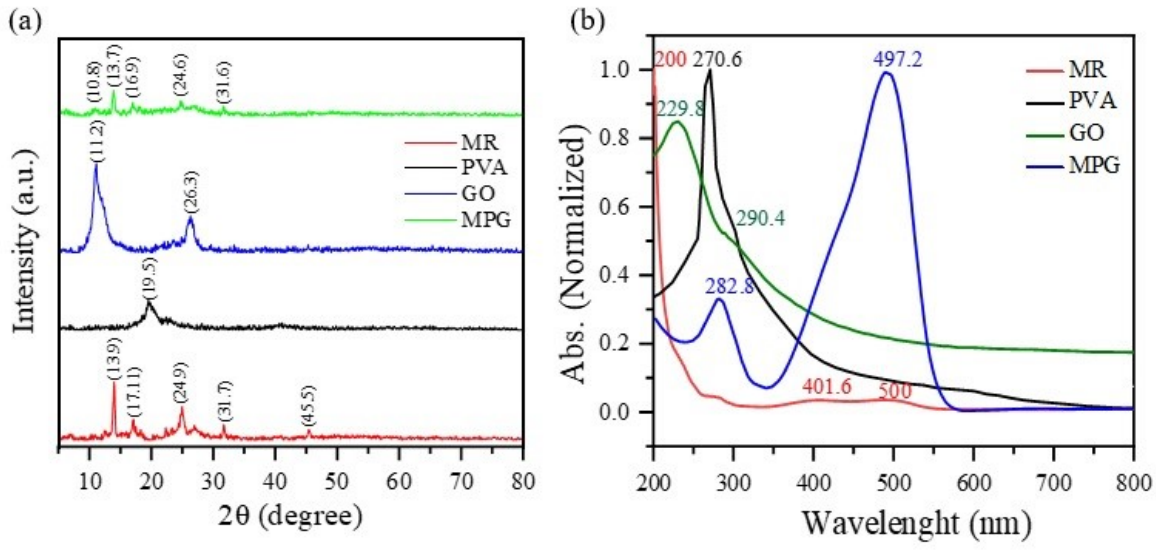

Figure S6: XRD analyses of MR, PVA, GO stand-alone, MPG composite, (b) Comparison of the electronic absorption spectra of MR, PVA, GO and MPG composite.